A high resolution geoid for the establishment of the GAVDOS multi-satellite calibration site

V.D. Andritsanos, G.S. Vergos, I.N. Tziavos
Department of Geodesy and Surveying, Aristotle University of Thessaloniki, Thessaloniki, Greece

E.C. Pavlis
Joint Center for Earth System Technology, JCET/UMBC, NASA Goddard Space Flight Center, Space Geodesy Branch, Greenbelt, Maryland, USA

S.P. Mertikas
Technical University of Crete, Mineral Resources Engineering Department, Chania, Crete, Greece

Abstract. The Topex/Poseidon (T/P) follow-on mission JASON-1 is planned to be launched by the end of 2000. A new multi-satellite calibration site has been proposed for the isle of Gavdos, south of the island of Crete, Greece. Part of the multi-satellite calibration experiment is the detailed computation of a high resolution geoid. The computed geoid is based on altimeter-derived, surface and shipborne gravity and height data. A currently available multi-satellite-based (GEOSAT-GM, ERS1-GM, ERS1-ERM, ERS2, T/P) altimetric geoid combined with newly available gravity data are used in the final model. New methods for the efficient combination of heterogeneous data are employed and special emphasis is paid to the *prediction error* estimates. We present the evaluation of the approximated accuracy estimates and the effect of the geoid error on the stability and reliability of the calibration site results. We will also elaborate on the assimilation of future measurements that are planned under the proposed project for the establishment of the calibration site.

Keywords. Satellite altimetry, sea gravimetry, sea surface heights, marine geoid, sea surface topography, MIMOST.

1 Introduction

Our study area is located in the Eastern Mediterranean region including the island of Crete and the isle of Gavdos, which is in the Southern part of Crete, Greece ($33^o \leq \varphi \leq 37^o$ and $21^o \leq \lambda \leq 29^o$). The island of Crete is situated parallel to the Hellenic Trench and only some 20km from the northern boundary of the trench line, where the Aegean microplate overthrusts the subducting African plate, thus indicating the special interest from the geodynamic point of view. Recent analysis of geodetic data, collected in the past two decades, indicate that Crete has one of the region's largest horizontal motions with respect to stable Europe (Smith et al., 1994; Le Pichon et al., 1995). The marine gravity data available for this region are poor in quality and accuracy. This study aims at the determination of a high accuracy geoid using all the available surface and satellite data. An attempt is also made to provide an accurate tool for the establishment of a multi-satellite calibration site in the isle of GAVDOS.

Altimetric Sea Surface Heights (SSHs) from the Geodetic Mission (GM) of GEOSAT and ERS1 satellites are used for the computation of the altimetric geoid solution. The TOPEX/POSEIDON (T/P) data are used for the validation of the computed solutions and belong to the six years (1992-1998) T/P altimetry mission. The marine free-air gravity anomalies were derived from the digitization of Morelli maps (Behrend et al., 1996). Additionally, mean sea gravity data from the GEOMED (GEOid in the MEDiterranean) project databank are used as well. The land free-air gravity anomalies used in our tests belong to the gravity and topographic databank established by Lagios et al. (1996).

2 Altimetric geoid

During the last few years satellite altimetry has provided numerous data for gravity field modeling with increasing accuracy. The geodetic missions cover earth densely and offer precise data sets due to the accurate models used for the geophysical corrections and the approximation of the satellite orbit. Thus, it is efficient to compute a marine geoid with an accuracy close to a few centimeters. The altimetric data sets used in this study were

GEOSAT-GM newly realized SSHs referred to JGM-3 (Joint Gravity Model – 3) orbits provided by Lillibridge (1999). The observation period of this data set was from 30th March 1985 – 30th September 1986. Additional altimetric data were those of ERS1-GM SSHs from AVISO (1998). The period of observation of these altimetric data was from 10th April 1994 to 21st March 1995. Finally, six years of T/P SSHs distributed by AVISO (1998) were used. The period of observation of this last data set was from 2nd October 1992 to 13th October 1998. Due to the limited test area the validation tests were first carried out in a larger area ($30^o \leq \varphi \leq 48^o$ and $0^o \leq \lambda \leq 40^o$) in order to compute representative outcomes.

2.1 Validation of GEOSAT-GM data

The GEOSAT-GM SSHs were in Geophysical Data Record (GDR) format and the application of the various geophysical and instrumental corrections were made in the first pre-processing step. The models and methods used are the same as those described in the GEOSAT-GM handbook (1997). In the present study the signal of the Sea Surface Topography (SST) was not taken into account due to unavailable external information about it. Thus, the corrected SSHs (174546 point values) are considered as geoid heights (N). GEOSAT data refer not only to sea but to some continental areas too, thus the first test had to deal with the removal of those data. A 1′×1′ bathymetric model for the Mediterranean Sea was used (Sandwell, 1996) and an interpolation of depth values was carried out in the points where SSHs from GEOSAT-GM were available. Then, data points with depths greater than –200m were neglected (see Table 1). According to this test 25855 point values (14.82%) were finally removed (see Table 1).

Table 1. GEOSAT-GM data before and after the bathymetry test. Unit: [m].

max	min	mean	std
240.151	-286.336	29.553	±13.323
240.151	-286.336	28.858	±13.428

After the bathymetry test the subtraction of the contribution of EGM96 (Lemoine et al., 1996) and GPM98b (Wenzel, 1998) geopotential models from the SSHs was made. The statistics of the derived geoid heights are summarized in Table 2.

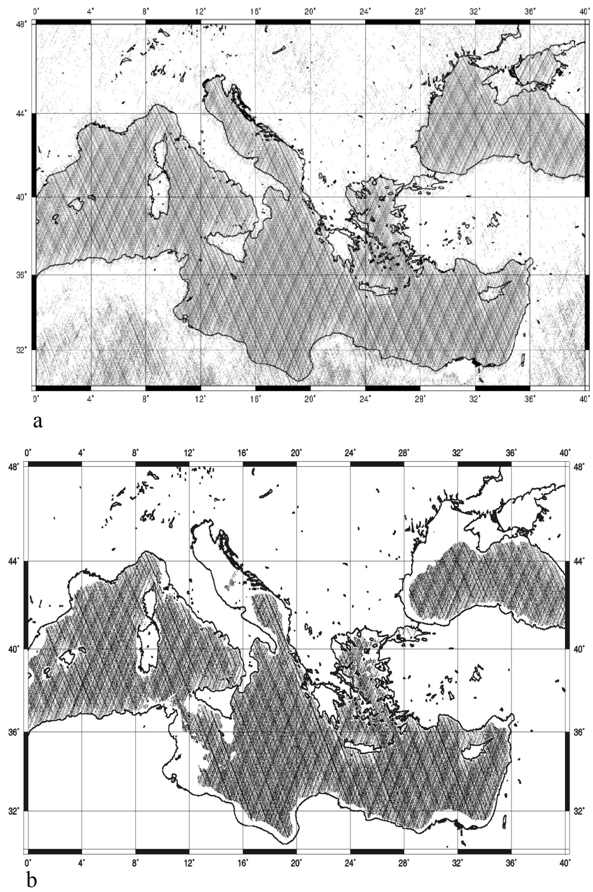

Fig. 1: GEOSAT-GM data distribution before (a) and after (b) the bathymetry test.

Table 2. GEOSAT-GM N_{res} to EGM96 and GPM98b geopotential models. Unit: [m]

	max	min	mean	std
N_{res} (EGM96)	212.341	-324.884	-0.473	±2.737
N_{res} (GPM98b)	212.823	-324.557	-0.502	±2.648

These first results of Table 2 show that the residual geoid heights include a number of unexpected values. This is due to the presence of blunders and/or systematic errors. In order to remove the aforementioned large values an additional 3*rms test for blunder detection was performed for the entire Mediterranean Sea. This resulted in the removal of 1926 residual geoid heights (1.3%) in the case of EGM96 and 1379 residual geoid heights (0.93%) in the case of GPM98b. Summarizing, during the validation tests (bathymetry and 3*rms) 27781 GEOSAT-GM geoid heights (15.9%) reduced to EGM96 geopotential model were removed and 27324 geoid heights (15.6%) reduced to GPM98b were eliminated.

The remaining residual geoid heights in the area under study (33°≤φ≤37° and 21°≤λ≤29°) are 18551 and 18595 for the reference surfaces of EGM96 and GPM98b, respectively. The statistics of these residual geoid heights in the test area are given in Table 3.

Table 3. GEOSAT-GM N_{res} to EGM96 and GPM98b geopotential models after the 3*rms test. Unit: [m]

	max	min	mean	std
$\mathbf{N_{res}}$ (EGM96)	1.261	-1.490	-0.337	±0.326
$\mathbf{N_{res}}$ (GPM98b)	1.482	-1.816	-0.773	±0.268

Comparing Tables 2 and 3 the refinement of the GEOSAT residual geoid heights is obvious. To the such derived residual geoid heights a crossover adjustment model was applied. Comparing the heights before and after adjustment non-significant improvement in terms of the standard deviation and the mean value of the differences was detected. This can be mainly attributed to the high quality of orbit determination of the GEOSAT-GM (JGM-3) altimetric data. For this reason in the subsequent numerical tests the residual geoid heights before adjustment were used.
In the next step the point residual geoid heights were transformed into a 5′×5′ grid. Then, restoring the contribution of EGM96 and GPM98b geopotential models to the residual geoid heights, the final geoid height solutions of GEOSAT-GM altimetry data were calculated (see Table 4).

Table 4. The final geoid solution from GEOSAT-GM altimetry data. Unit: [m]

	max	min	mean	std
N (EGM96)	38.102	0.670	16.587	±9.683
N (GPM98b)	38.186	0.672	16.626	±9.708

2.2 Validation of ERS1-GM data

The ERS1-GM SSHs were corrected due to the geophysical and instrumental errors (AVISO, 1998). Then from the corrected SSHs the contribution of the EGM96 and GPM98b geopotential models was removed. The statistics of the such derived residual geoid heights are shown in Table 5.

Table 5. ERS1-GM N_{res} to EGM96 and GPM98b geopotential models. Unit: [m]

	max	min	mean	std
$\mathbf{N_{res}}$ (EGM96)	1.572	-2.062	-0.223	±0.347
$\mathbf{N_{res}}$ (GPM98b)	2.832	-1.893	-0.236	±0.484

In order to further detect remaining outliers an additional 3*rms test was applied to aforementioned residual geoid heights. The statistical results of this numerical test are summarized in Table 6. As it has been mentioned for the GEOSAT-GM residual geoid heights, a further crossover adjustment to the data derived was not necessary.

Table 6. ERS1-GM N_{res} to EGM96 and GPM98b geopotential models after the 3*rms test. Unit: [m]

	max	min	mean	std
$\mathbf{N_{res}}$ (EGM96)	1.095	-1.180	-0.264	±0.317
$\mathbf{N_{res}}$ (GPM98b)	1.016	-1.400	-0.711	±0.267

The data after 3*rms test were used for the prediction in a 5′×5′ grid. In this gridded residual geoid heights the contribution of the geopotential models was restored. The statistics of the such derived geoid height solutions are given in Table 7. For a better visualisation procedure 2-D representations of the complete geoid solutions are depicted in Figures 2 and 3.

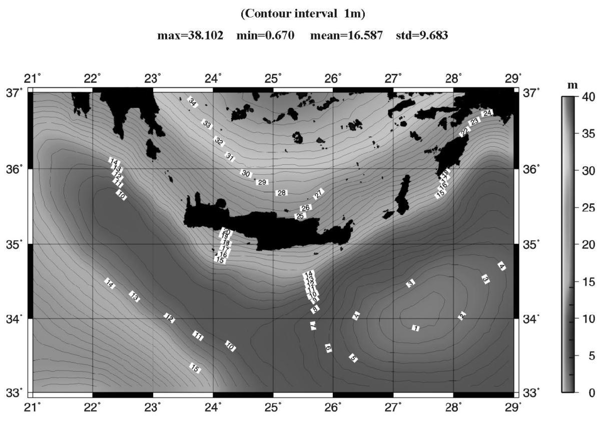

Fig. 2: The final geoid solution from GEOSAT-GM to EGM96 reference surface.

Table 7. The final geoid solution from ERS1-GM altimetry data. Unit: [m]

	max	min	mean	std
N (EGM96)	37.978	0.726	16.677	±9.688
N (GPM98b)	38.107	0.714	16.697	±9.697

3 Gravimetric geoid

The gravity data used were sea and land free-air gravity anomalies in the area under study. More analytically, 30437 sea free-air gravity anomalies were digitized from Morelli maps (Behrent et al., 1996), 596 land free-gravity anomalies were collected from Lagios et. al. (1996) databank and 1813 5′×5′ sea free-air gravity anomalies were extracted from the GEOMED project databank. All these gravity data values were first reduced to EGM96 and GPM98b reference surfaces.

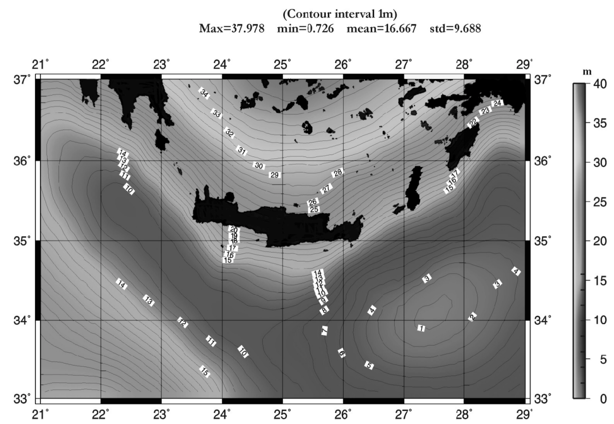

Fig. 3: The final geoid solution from ERS1-GM to EGM96 reference surface.

The such derived residual gravity anomalies were gridded in a 5′×5′ grid and the computation of the residual geoid heights was carried out by applying the 1-D spherical FFT method (Haagmans et al., 1993). The statistics of these residual geoid heights are reported in Table 8.

Table 8. Gravimetric residual geoid heights to EGM96 and GPM98b reference surfaces. Unit: [m]

	max	min	mean	std
N_{res} (EGM96)	1.702	-2.273	0.009	±0.591
N_{res} (GPM98b)	1.924	-1.845	-0.243	±0.527

The final gravimetric geoid solutions are then calculated by restoring the contribution of the reference models EGM96 and GPM98b to geoid height residuals. The statistics of these solutions are pointed out in Table 9. Furthermore, the complete geoid solution with respect to EGM96 is presented in Figure 4.

Table 9. The final gravimetric geoid solution to EGM96 and GPM98b reference. Unit: [m]

	max	min	mean	std
N (EGM96)	38.044	2.093	16.997	±9.332
N (GPM98b)	38.134	2.263	17.102	±9.279

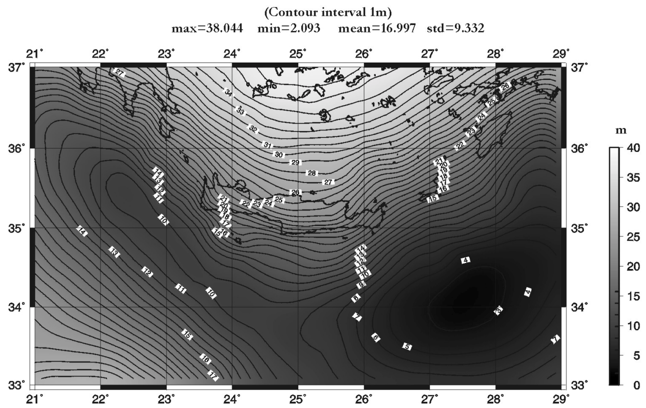

Fig. 4: The final gravimetric geoid solution to EGM96 reference surface.

4 Combined geoid solution

From the altimetric and gravimetric solutions described in the previous sections combined solutions were determined using the Multiple Input – Multiple Output System Theory (MIMOST) presented by Andritsanos (2000), Andritsanos et. al. (2000a). The data used are the altimetric geoid heights from ERS1-GM reference to EGM96 and GPM98b models and the corresponding gravimetric geoid solutions. Due to the lack of specific information about the errors in both altimetric and gravimetric solutions, simulated noises were used as input error. Randomly distributed fields were generated using 5cm standard deviation for the altimetric data and 7cm standard deviation for the gravimetric one. It is noticing that in the case of repeat altimetric missions an estimation of the input error Power Spectral Density PSD function can be evaluated directly using this successive information (Andritsanos et. al., 2000b). The final solutions as well as the error PSD function, of the MIMOST method were calculated according to the following equations:

$$\hat{N}_o = \begin{bmatrix} H_{\hat{N}N_g} & H_{\hat{N}N_a} \end{bmatrix} \left(\begin{bmatrix} P_{N_{og}N_{og}} & P_{N_{og}N_{oa}} \\ P_{N_{oa}N_{og}} & P_{N_{oa}N_{oa}} \end{bmatrix} - \begin{bmatrix} P_{m_g m_g} & 0 \\ 0 & P_{m_a m_a} \end{bmatrix} \right) \begin{bmatrix} P_{N_{og}N_{og}} & P_{N_{og}N_{oa}} \\ P_{N_{oa}N_{og}} & P_{N_{oa}N_{oa}} \end{bmatrix}^{-1} \begin{bmatrix} N_{og} \\ N_{oa} \end{bmatrix} \tag{3}$$

$$P_{\hat{e}\hat{e}} = \Bigg\{ \begin{bmatrix} H_{\hat{N}N_g} & H_{\hat{N}N_a} \end{bmatrix} \left(\begin{bmatrix} P_{N_{og}N_{og}} & P_{N_{og}N_{oa}} \\ P_{N_{oa}N_{og}} & P_{N_{oa}N_{oa}} \end{bmatrix} - \begin{bmatrix} P_{m_g m_g} & 0 \\ 0 & P_{m_a m_a} \end{bmatrix} \right) - \begin{bmatrix} \hat{H}_{\hat{N}_o N_{og}} & \hat{H}_{\hat{N}_o N_{oa}} \end{bmatrix} \begin{bmatrix} P_{N_{og}N_{og}} & P_{N_{og}N_{oa}} \\ P_{N_{oa}N_{og}} & P_{N_{oa}N_{oa}} \end{bmatrix} \Bigg\} \tag{4}$$
$$\left(\begin{bmatrix} H^{*}_{\hat{N}N_g} \\ H^{*}_{\hat{N}N_a} \end{bmatrix} - \begin{bmatrix} \hat{H}^{*}_{\hat{N}_o N_{og}} \\ \hat{H}^{*}_{\hat{N}_o N_{oa}} \end{bmatrix} \right) + \begin{bmatrix} \hat{H}_{\hat{N}_o N_{og}} & \hat{H}_{\hat{N}_o N_{oa}} \end{bmatrix} \begin{bmatrix} P_{m_g m_g} & 0 \\ 0 & P_{m_a m_a} \end{bmatrix} \begin{bmatrix} H^{*}_{\hat{N}N_g} \\ H^{*}_{\hat{N}N_a} \end{bmatrix}$$

where $\hat{N}_o$ is the combined geoid estimation, N_g and N_a are the pure gravimetric and altimetric signals respectively, N_{og} and N_{oa} are the gravimetric and altimetric observations, m_g and m_a are the input noises, H_{xy} is the theoretical operator that connects the pure input and output signals, $\hat{H}_{x_o y_o}$ is the optimum frequency impulse response function, and $P_{\hat{e}\hat{e}}$ is the error PSD function.

The final geoid height solutions from the common adjustment of the heterogeneous heights referenced to the EGM96 and GPM98b geopotential models can be seen in the figure 5.

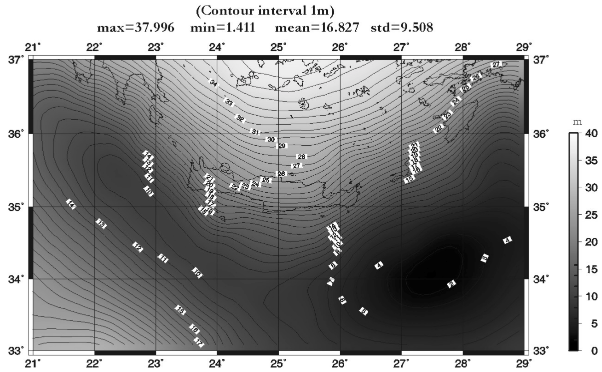

a

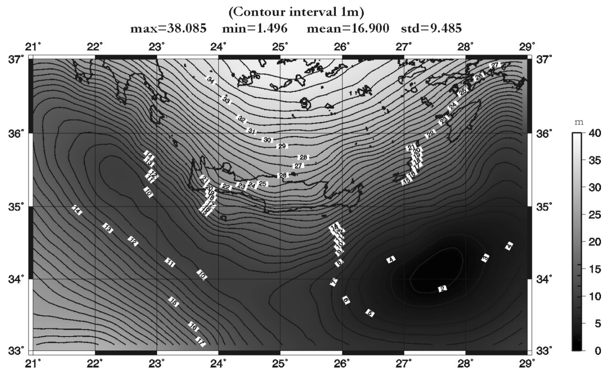

b

Fig. 5: The final geoid height solutions from the MIMOST method to EGM96 (a) and GPM98b (b) reference surfaces.

5 Comparison of different geoid height solutions and T/P SSHs

The previous described geoid height solutions are intercompared and also compared with T/P SSHs, which are considered as geoid heights when neglecting the SST signal. Largest discrepancies were detected when comparing gravimetric and altimetric solutions. This can be mainly credited to the low accuracy of the available gravimetric data sets as well as to the absence of the SST signal in the gravimetric solutions. In particular in the eastern part of the area under study, where GEOMED free-air gravity anomalies were used, significant differences between the gravimetric solution and the corresponding altimetric one (ERS1-GM, EGM96) were detected (See Figure 6).

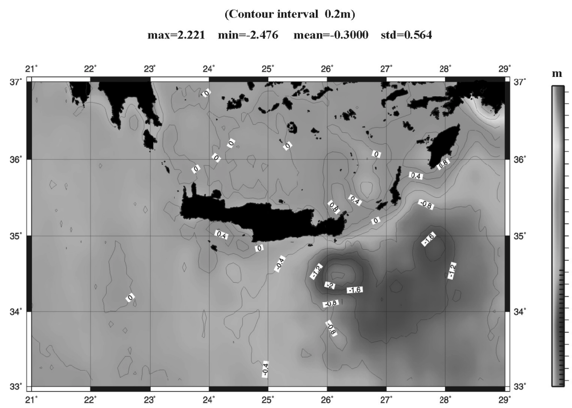

Fig. 6: Differences between gravimetric geoid height solution and ERS1-GM one to EGM96.

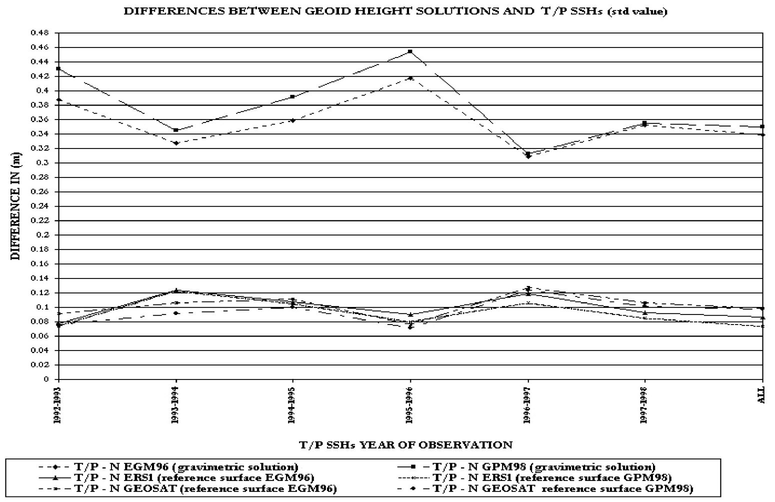

Fig. 7: Standard deviation of differences between stacked T/P data and geoid height solutions.

Some comparisons between the aforementioned solutions and the SSHs from T/P mission were also carried out. The computed differences were minimized by using a four-parameter transformation model:

$$SSH_{TOPEX/POSEIDON} = N - b_o \cos\phi \cos\lambda - \\ - b_1 \cos\phi \sin\lambda - b_2 \sin\phi - b_3 \quad (5)$$

where the parameters b_o, b_1, b_2 and b_3 were calculated by a least squares technique and N is the altimetric or gravimetric geoid height depending on the solution under consideration. Comparing the standard deviation of the differences between the different geoid height solutions and the stacked T/P heights, for each year as well as for the entire period (1992-1998), it is concluded that the altimetric solutions are superior to the gravimetric ones. These differences reach the level of 40cm in terms of standard deviation and are outlined in figure 7. The comparison between the common adjusted geoid heights and the stacked T/P SSHs (3rd year) present an accuracy close to 18cm in terms of standard deviation of the differences (see figure 8). Additionally, when comparing the pure altimetric geoid heights with the T/P SSHs the accuracy varies between the level of 7cm and 11cm in terms of standard deviation of the corresponding differences (see also figure 7).

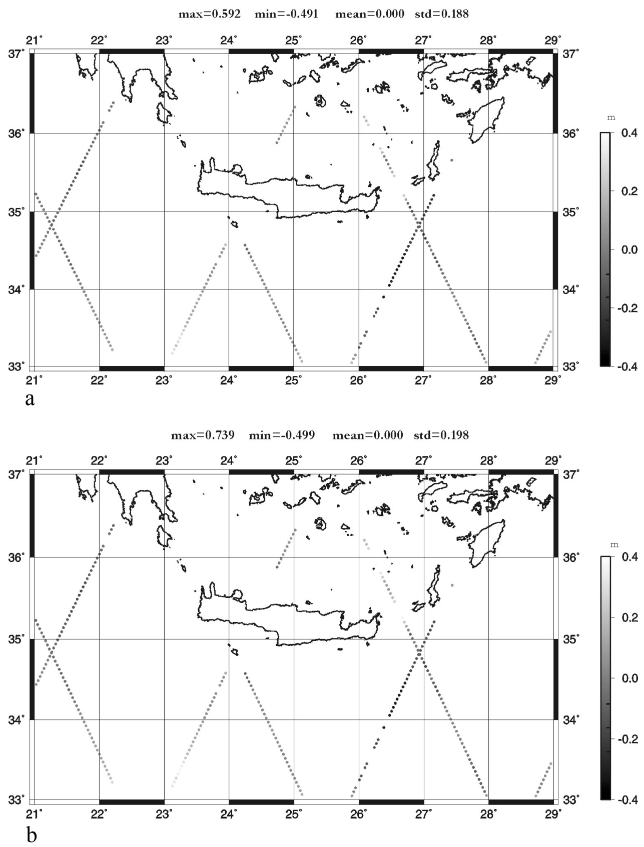

Fig. 8: Differences between the final geoid height solutions from the MIMOST method to EGM96 (a) and GPM98b (b) reference models and the stacked T/P SSHs (3rd year).

6 Conclusions – Future plans

Eight local geoid solutions are computed for the Crete area in Southern Greece. Altimetric and sea and land gravimetric data are used for the optimal determination of an accurate geoid solution in the area under study. The method used to derive the pure altimetric and gravimetric solutions is the remove-restore technique. In order to compute the gravimetric residual geoid heights the 1-D FFT method is used. Finally, the combined solutions are evaluated using the Multiple Input Multiple Output System Theory.

According to the validation procedures the computation of pure altimetric geoid with an accuracy close to 5cm could be achieved in the region of Crete. The corresponding gravimetric solutions present low accuracy results since they are strongly influenced by the inefficiency of the available free-air gravity anomalies. The differences between the altimetric and the gravimetric solutions present a standard deviation close to 40cm caused by the absence of the SST signal in the gravimetric solutions and the limited accuracy of the gravity data.

T/P SSHs can be used as geoid heights for validation purposes. Geoid heights derived from altimetry data show smaller differences, than the gravimetric ones, when compared with T/P SSHs. Additionally the common adjusted geoid heights using the MIMOST method show wicker accuracy than the altimetric geoid heights when compared with T/P SSHs heights. This is due to the use of low accuracy gravity data in the MIMOST method.

In order to obtain a higher resolution and higher accuracy geoid solution in the test area a significant improvement of both land and sea gravity databases is necessary. It is expected that the forthcoming gravity field dedicated satellite missions will contribute to the improvement of such databases. New GPS/leveling data in the insular complex will contribute to the stability of the future geoid solutions. The achieved accuracy of 5cm in the altimetric solutions combined with GPS observations provide a suitable level of accuracy for the establishment of the GAVDOS multi-satellite calibration site.

Acknowledgements

The financial assistance provided to the first author by the Hellenic National Scholarship Foundation is gratefully acknowledged. We extensively used the Generic Mapping Tools Version 3.1 (Wessel and Smith, 1998) in displaying our results.

References

Andritsanos, V.D., *Optimum combination of terrestrial and satellite data with the use of spectral techniques for applications in geodesy and oceanography*. PhD dissertation, School of Rural and Surveying Engineering, Faculty of Engineering, Aristotle University of Thessaloniki, Department of Geodesy and Surveying, 2000.

Andritsanos, V.D., M.G. Sideris and I.N. Tziavos. *A survey of gravity field modelling applications of the Input-Output System Theory (IOST)*. To appear in IGeS Bulletin, 2000a.

Andritsanos, V.D., M.G. Sideris and I.N. Tziavos. *Quasi-stationary Sea Surface topography estimation by the multiple Input-Output method*. Accepted for publication in Journal of Geodesy, 2000b.

AVISO User Handbook – Corrected Sea Surface Heights (CORSSHs). AVI-NT-011-311-CN, Edition 3.1, 1998.

Behrend, D., H. Denker, and K. Schmidt. *Digital gravity data sets for the mediterranean sea derived from available maps*. Bulletin d' information, No 78, pp. 31-39, BGI, 1996.

The Geosat Altimeter JGM-3 GDRs Handbook. Internet Resources:http://www.ibis.gdrl.noss.gov/SAT/gdrs/geosat-handbook, 1997.

Haagmans, R., E. de Min and M. van Gelderen. *Fast evaluation of convolution integrals on the sphere using 1D FFT, and a comparison with existing methods for Stokes' integral*. Manuscr. Geod. 18, pp. 227-241, 1993.

Lagios, E., S. Chailas and R.G. Hipkin. Newly compiled gravity and topographic databanks of Greece. *Geophys. J. Int.*, 126, 287-190, 1996.

Lemoine, F.G., et al. *The development of the join NASA GSFC and NIMA geopotential model EGM96*, NASA Technical Paper, 1998 – 206861, 1998.

Lillibridge, J., The GEOSAT-GM Altimeter JGM-3 GDRs, personal communication, 1999.

Sandwell D. *Data Base Description for Digital Bathymetric Data Base-Variable Resolution (DBDB-V)*. Version 1.0, Naval Oceanographic Office, Stennis Space Center, March, 1996

Smith D.E., R. Kolenkiewicz, J.W. Robbins, P.J. Dunn, M.H. Torrence. Horizontal crustal motion in the Central and Eastern Mediterranean inferred from Satellite Laser Ranging measurements. *Geophysical Research Letter*, 21, 1979 – 1982, 1994b.

Pichon Le, X.J. Angelier, N. Chamot-Rooke, S. Lallemant, R. Noomen, G. Veis, Geodetic determination of the kinematics of Central Greece with respect to Europe: Implications for Eastern Mediterranean Tectonics. *Journal of Geophysical Research*, 100, 12265-12690, 1995.

Vergos, G.S., *The contribution of satellite altimetry to gravity field modeling – A case of study in the Eastern Mediterranean*. Diploma thesis, School of Rural and Surveying Engineering, Faculty of Engineering, Aristotle University of Thessaloniki, Department of Geodesy and Surveying, 2000.

Wenzel, H.G. *Global models of the gravity field of high and ultra-high resolution*. In Lecture Notes of IAG's Geoid School, Milano, Italy, 1999.

Wessel, P., and W.H.F. Smith. *New improved version of Generic Mapping Tools released*. EOS Trans. Amer. Geophys. U., vol. 79 (47), pp. 579, 1998.